Journal of Southeast University (English Edition) Vol. 27, No. 4, pp. 410 – 416 Dec. 2011 ISSN 1003—7985

Electromagnetic simulation and experimental analysis of microwave heaters for asphalt pavements

Zhu Songqing[1,2] Zhang Zhisheng[1] Shi Tailong[3]

([1]School of Mechanical Engineering, Southeast University, Nanjing 211189, China)
([2]School of Automation, Nanjing Institute of Technology, Nanjing 211167, China)
([3]School of Information Science and Engineering, Southeast University, Nanjing 211189, China)

Abstract: In order to study the thermoelectric efficiency of microwave heating and reproduction of asphalt pavements and the uniformity of reproduction temperature distribution, a waveguide excitation cavity is designed and applied to the structural design of a microwave heater. The structural sizes of the incentive cavities are determined based on the waveguide transmission line theory. Using IE3D software, electromagnetic simulations are respectively carried out in four different situations, including the distances between the magnetron probes (antennas) and a short-circuit board, different horn electric lengths and aperture sizes, different dielectric properties of the asphalt mixture, and the distances between the asphalt surface and the mouth cavity. The results show that, when the distance between the magnetron probe and the short-circuit board is 32.5 mm, it is the best installation site; reduction of aerial length is the main factor in improving the heating uniformity. When the aggregate is limestone, the best heating effect can be produced. Maximum radiation efficiency can be realized by adjusting the space between the heater radiation port and the asphalt pavement. The experimental results of asphalt mixture heating in four different situations have a substantial agreement with the simulation results, which confirms that the developed microwave heater can achieve better impedance matching, thus improving the quality and efficiency of heating regeneration.

Key words: microwave heater; excitation cavity; structural design; electromagnetic simulation; temperature distribution; experimental analysis

doi: 10.3969/j.issn.1003 – 7985.2011.04.013

In China, a combination of microwave heating techniques and hot in-place reheating regeneration has currently become an important, hot in-place recycling (HIPR) technology, and has attracted more and more attention[1]. A main issue in developing a microwave heating recycling system is the design of radiation antennas. The antenna should provide a uniform radiation distribution to achieve uniform heating on the surface of asphalt mixtures and eliminate tangential hot-spots and cold-spots on the surface. This will increase the efficiency and quality of recycling, and meanwhile achieve optimal matching of impedance[2].

Received 2011-06-20.

Biographies: Zhu Songqing (1969—), male, doctor; Zhang Zhisheng (corresponding author), male, doctor, professor, oldbc@seu.edu.cn.

Foundation items: The Sci-Tech Achievements Transformation Program of Colleges and Universities in Jiangsu Province (No. JH09-13), the Research Fund of Nanjing Institute of Technology (No. YKJ201005).

Citation: Zhu Songqing, Zhang Zhisheng, Shi Tailong. Electromagnetic simulation and experimental analysis of microwave heaters for asphalt pavements[J]. Journal of Southeast University (English Edition), 2011, 27(4): 410 – 416. [doi: 10.3969/j.issn.1003 – 7985.2011.04.013]

In practical applications, the microwave source of the radiant heater is generated by a continuous wave magnetron. The magnetron can directly drive rectangular waveguides with high transmission efficiency, and have a high load resistance capacity and a high resistance to thermal loads[3]. When asphalt pavement is heated by using a magnetron, as a monopole antenna, the magnetron antenna in the excitation cavity should be used to encourage producing a high-frequency electric field to radiate the microwave energy[4-5]. Therefore, when the configuration of a microwave radiation heater is designed, an excitation cavity chamber must be added to the upper part of the speaker cone radiation angle, and the excitation cavity forms a rectangular waveguide chamber with the size of $a \times b$.

1 Structural Design of Excitation Cavity

According to the waveguide transmission theory, the electric field distribution in the waveguide broadside is shown in Fig. 1 and its maximum intensity is in a wide-brimmed center. There are many wave modes in the rectangular waveguide and the main mode is TE_{10}. In order to excite a basic waveform TE_{10} mode in the waveguide, the magnetron (antenna) should be stretched into the center of the waveguide broadside[6], and in order to make a one-way microwave transmission in the waveguide, one end of the waveguide should result in a short circuit. According to the structure and installation requirements of the magnetron, the magnetron antenna axis is perpendicular to the asphalt pavement. From the antenna radiation theory, we know that radiation is directional, and the radiation intensity perpendicular to the antenna axis direction is the highest. Therefore, a transition metal surface must be designed on the other end to take the corner reflection of the transmission direction of the electromagnetic waves reflected to the other end, in order to achieve its vertical radiation on the pavement. Its transmission direction is indicated in Fig. 2.

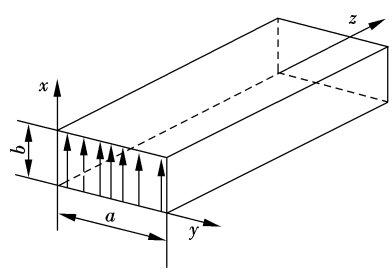

Fig. 1 Waveguide broadside electric field distribution

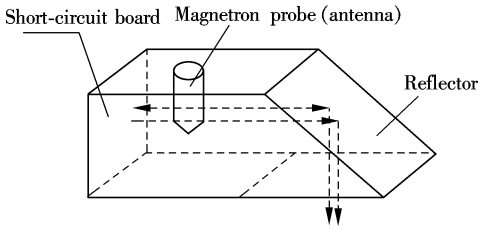

Fig. 2 Microwave transmission direction in excitation cavity

For a waveguide system used as energy transmission, the following principles are generally followed to determine the waveguide cross-section sizes: 1) Single mode operation is ensured and a band width is as wide as possible; 2) Breakdown power (i. e. power capacity) is as large as possible; 3) Loss or attenuation is as little as possible.

Waveguide cutoff wavelength λ_c is defined as

$$\lambda_c = \frac{2}{\sqrt{(m/a)^2 + (n/b)^2}} \tag{1}$$

where m and n are the semi-cycles of the cross-section long side and short side of the rectangular waveguide, respectively.

According to the first design principle mentioned above, only a transmission single mode TE_{10} is considered. On the one hand, the working wavelength should meet $\lambda < \lambda_{cTE_{10}} = 2a$, which is a pass-through condition of the microwave; on the other hand, the working wavelength should meet the first higher harmonic mode $\lambda > \lambda_c$, which is a rejection condition. Based on the relative sizes of a and b, the first higher harmonic mode may be the mode TE_{20}, and the corresponding cut-off wavelength is a; the first higher harmonic mode may be mode TE_{01}, and the corresponding cut-off wavelength is $2b$. In order to make a single mode workspace band as wide as possible, $a \geqslant 2b$ should be satisfied, and by comprehensive consideration, the a and b ranges are

$$a = 0.7\lambda, \quad b = (0.4 \text{ to } 0.5)a \tag{2}$$

According to the second design principle, the waveguide transmission power cannot lead to puncture because of insufficient power capacity; therefore, power capacity must be considered when the excitation waveguide is designed. The power capacity of the waveguide transmission of mode TE_{10} is calculated as

$$P_c = \frac{abE_m^2}{4Z_{TE_{10}}} = \frac{abE_c^2\sqrt{1-(\lambda/(2a))^2}}{480\pi} \tag{3}$$

where E_c is the strength of the air puncture electric field in the waveguide and it is equal to 3×10^6 V/m. In order to ensure that no waveguide puncture is produced and only mode TE_{10} is transmitted, $0.5 < \lambda/(2a) < 0.9$ must be satisfied. Then, we have

$$0.56\lambda < a < \lambda \tag{4}$$

According to the third design principle, in order to prevent too much loss in microwave power through waveguide excitation, the principle of minimum loss or attenuation must be taken into account. The decay constants formula in transmission mode TE_{10} is shown as

$$\alpha_c = \frac{R_s[1+(2b/a)(\lambda/(2a))^2]}{120\pi b\sqrt{1-(\lambda/(2a))^2}} \tag{5}$$

where R_s is the resistance of the dielectric surface. According to Eq. (5), b should be chosen to be as great as possible. Based on the three design principles, a and b can be chosen as

$$\frac{\lambda}{2} < a < \lambda, \quad 0 < b < \frac{\lambda}{2}, \quad b \leqslant \frac{a}{2} \tag{6}$$

According to Eq. (6), $a = 90$ mm, $b = 40$ mm are chosen first. Based on the above-mentioned design principles, two structural types are designed as follows. One is the modular style; that is, the surfaces of excitation cavity waveguide and pyramidal horn radiation are combined to assemble the two together to form a radiant heat chamber with a modular configuration as shown in Fig. 3(a). The other is the integral style; that is, excitation chambers are formed into a whole through a waveguide transition and a pyramidal horn, with its structural design shown in Fig. 3(b).

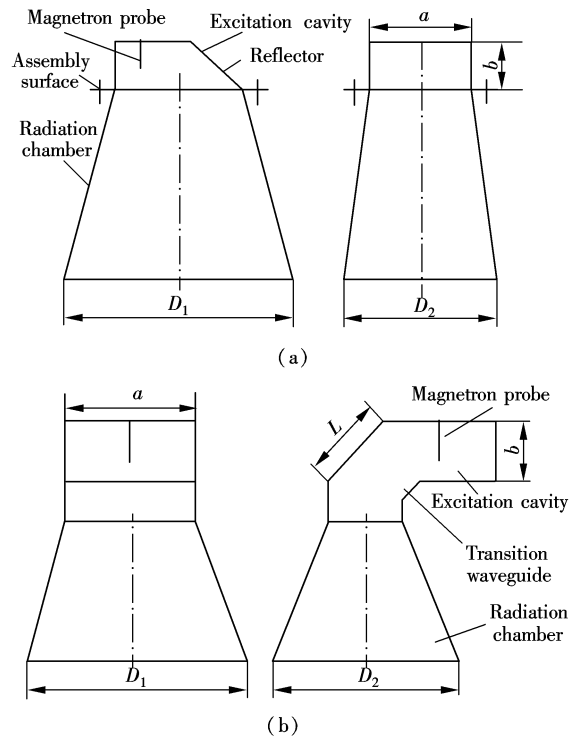

Fig. 3 Sketch of two structural types. (a) Modular configuration; (b) Integral configuration

The excitation cavity of the integral configuration can be designed as an E-plane double-angle-connection off-switch structure, and a waveguide transition with the length of L is added in the middle of the waveguide head face in both directions as shown in Fig. 3(b). In order to completely offset the reflected waves of two waveguide connectivity ports, L should be equal to the odd multiples of the waveguide wavelength; that is,

$$L = \frac{(2n+1)\lambda_g}{4} \qquad n = 0, 1, 2, \ldots \tag{7}$$

where λ_g is the waveguide wavelength. For a single-mode transmission waveguide,

$$\lambda_g = \frac{2a\lambda}{\sqrt{4a^2 - \lambda^2}} \tag{8}$$

Taking $\lambda = 12.2$ cm, $a = 9$ cm, $n = 0$ and $n = 1$ into Eqs. (7) and (8), we can obtain $L_1 = 4.15$ cm and $L_2 = 12.44$ cm.

The aperture size can take two groups of dimensions, with the upper limits $D_1 = 15$ cm and $D_2 = 12$ cm and the lower limits $D_1 = 12$ cm and $D_2 = 10$ cm; the height of the radiation chamber c can take a value of 5 to 15 cm. For the modular structure, c can take its maximum; for the integral structure, c can take its minimum. After the installation of the electromagnetic probes, modular and integral actual structures are shown in Fig. 4.

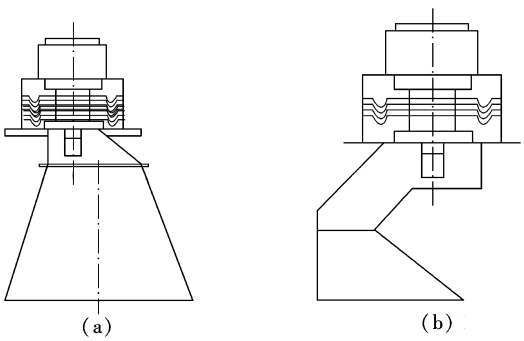

Fig. 4 Actual structure of two structural types. (a) Modular configuration; (b) Integral configuration

2 Geometric Modeling and Simulation Optimization

2.1 Modeling conditions and structural modeling

Correct modeling conditions and appropriate assumptions should simulate to the greatest degree actual working situations, which are the basis for simulation optimization:

1) According to the Zeland user's manual[7], the cylindrical antenna in the electromagnetic probe can be replaced by a thin strip antenna, since there is a minimal difference between the simulation results of these two methods.

2) The distance between the feed end and the grounded layer is 1 mm, and the actual measured length of the magnetron-tube antenna is 22 mm.

3) A 50 Ω normalized incident wave source is defined as a 10 mW incident wave.

4) The relative dielectric constant of the asphalt mixture $\varepsilon'_r = 5.8$, the dielectric loss $\tan\delta = 0.034\,4$, the relative permeability $\mu' = 1$; and the magnetic loss $\tan\delta_e = 0$. The thickness of asphalt $H = 120$ mm, which is a semi-infinite flat medium to fill in all the air in the radiation direction.

5) The operation frequency of a 2M210F type magnetron is 2.455 GHz, so the initial simulation frequency is 2.43 GHzand the end frequency is 2.48 GHz. The simulation frequency step is 0.5 MHz.

6) The highest frequency of discrete parameters is 2.5 GHz. Each wave length has 10 units.

7) The initial distance h between the horn aperture and the asphalt mixture sample is 80 mm. The structural modeling of the two types of microwave heaters is shown in Fig. 5.

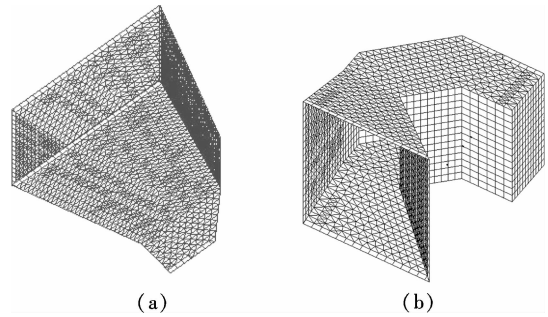

Fig. 5 Geometric modeling of two structural types. (a) Modular heater; (b) Integral heater

As there is a second leakage problem in the assembly surfaces of the excitation cavity and the radiation chamber of the modular structure, considering the actual production process, an integral structure is used in the actual heating cavity. Therefore, the following simulation optimization and experiments are carried out on the basis of the integral structure.

2.2 Simulation Optimization and Result Analysis

2.2.1 Effects of distances between magnetron probe and short-circuit board on radiation performance

Suppose that the characteristic impedance between the magnetron antenna and the short-circuit board is Z_c, the input impedance is Z_{in}, the characteristic impedance from the antenna transmission direction to the asphalt mixture sample is Z', and the load impedance from the antenna to the asphalt sample is Z_L. According to the transmission line theory, we obtain

$$Z_L = \frac{Z_{in}Z'}{Z_{in} + Z'} \tag{9}$$

$$Z_{in} = jZ_c\tan(\beta z) = jZ_c\tan(\beta l) \tag{10}$$

where β is the microwave phase shift constant and $\beta = 2\pi/\lambda$. Then the reflection coefficient is

$$\Gamma = \frac{Z_L - Z_c}{Z_L + Z_c} \tag{11}$$

Substituting Eqs. (9) and (10) into Eq. (11), we can know that Γ is closely related to the distance l between the antenna and the short-circuit board. It is confirmed that when the insertion depth of the magnetron antenna is constant, the minimum reflection coefficient can be obtained through adjusting distance l between the antenna and the short-circuit board so as to achieve the best excitation.

The coordinate system as shown in Fig. 6 is established. According to the waveguide theory, the maximum strength of the waveguide broadside will be achieved at the center $y = 0$ of the electric field, so the magnetron probes can only move along the z direction. At the same time, when the space between the magnetron installation location and the short-circuit board is equal to a 1/4 wavelength, a pure standing wave will be formed as shown in Fig. 7. Therefore, the initial simulation position is $l = 1/(4\lambda)$, that is, at the x-z plane center (0, 30.5 mm). Taking into account the

surface size and the magnetron assembly mounting-hole size, parallel movement along the z axis in steps of 2 mm from left to right is used to determine the best installation location of the magnetron probes.

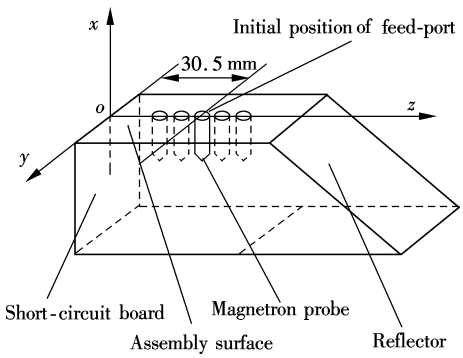

Fig. 6 Location position of magnetron probe

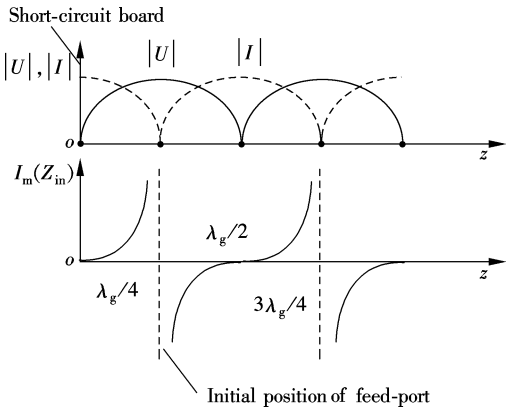

Fig. 7 Curves of voltage and current vs. impedance at pure standing wave

The radiation performance of a heating cavity at five kinds of installation locations is shown in Tab. 1.

Tab. 1 Radiation performance of heating cavity at different installation positions of probes at 2.455 GHz

Pattern parameters	Installation location l/mm				
	26.5	28.5	30.5	32.5	34.5
Input power/mW	1.634 6	1.944 1	1.992 2	2.346 4	2.229 9
Radiated power/mW	1.634 6	1.944 1	1.992 2	2.346 4	2.229 9
Radiation efficiency/%	100	100	100	100	100
Linear gain/dBi	3.455 9	4.171 6	4.345 3	4.196 1	4.231 9
Coefficient of linear direction/dBi	11.321 9	11.284 9	11.352 1	10.492 1	10.749 0
3 dB beam bandwidth/(°)	(6.126 0, 55.754 7)	(6.118 4, 55.606 5)	(6.114 9, 55.911 2)	(6.394 0, 56.900 0)	(6.198 3, 56.040 1)

In the simulation model, an integral heater with l of 32.5 mm is used, and the distance h between the heater and the road is 80 mm. According to the simulation results, we can know that when the incident power is the same, the five locations can meet a radiation efficiency of 100%. When the space l between the installation location of the magnetron probe and the short-circuit board is 32.5 mm, input power and radiated power are at their maximums, and the linear gain and the coefficient of the linear direction are at their minimums. When the 3dB bandwidth of the beam is at its maximum, the position should be the best magnetron installation location. Taking into account the production processes, when the installation location is between 31.5 and 33.5 mm, the requirements can be met.

2.2.2 Effects of different horn lengths and aperture sizes on radiation performance

Any size heater which satisfies the design principles can be selected as the basis type. Simulations are carried out for different horn lengths and aperture sizes, and the results are shown in Tab. 2.

From Tab. 2, it can be seen that on the premise of constant size of the horn aperture, shortening the horn antenna length is a key factor in reducing gains, increasing beam width and improving the heating uniformity. When the aperture size becomes smaller and the antenna length is constant, the standing wave ratio decreases, while radiation efficiency is increased. Under the same conditions, shortening the antenna length is better than reducing the aperture size.

Tab. 2 Radiation performance of heating cavity of different horn lengths and aperture sizes at 2.455 GHz

Pattern parameters	Prototype	Shortened horn length and the same aperture size	Shortened aperture size and the same horn length
Input power/mW	1.676 7	1.740 0	1.696 2
Radiated power/mW	1.676 7	1.740 0	1.696 2
Radiation efficiency/%	100	100	100
Linear gain/dBi	2.132 3	2.128 2	1.925 3
Coefficient of lineardirection/dBi	9.887	9.723 2	9.630 5
3 dB beam bandwidth/(°)	(6.576, 53.426)	(17.560, 54.262)	(17.775, 54.939)

2.2.3 Effects of different dielectric properties of asphalt mixture on radiation performance

Microwave heating uses heat dissipation into the material to realize the temperature rise, and its ability to absorb microwaves is different when the properties of the materials are different[8], so the dielectric loss should be considered in the design of the microwave cavity body of a microwave heater. The bitumen cutting angle of dielectric loss is very low (approximately equal to 0.001[9]) and basically does not absorb microwaves. So, the aggregate-asphalt mixture is only considered. The radiation simulations of diorite, limestone, and quartz aggregate asphalt mixtures are carried out, and the results are shown in Tab. 3.

An integral heater with l of 32.5 mm is used in the simulation model, and its distance to the road is 80 mm. From the simulation results, the radiation efficiency of three different aggregates is 100%, and their input power and radiated power are basically the same. The limestone aggregate has the strongest microwave absorption ability, which leads to the best heating results. Compared with limestone and diorite aggregates, the linear gain and the linear direction coefficient of the quartz aggregate are greater, indicating that its absorption capacity is smaller. It is comprehensively considered that this kind of heater has a higher frequency band, which can adapt to the requirements of a variety of aggregates.

Tab. 3 Radiation performance of heating cavity of asphalt mixture with different dielectric properties

Pattern parameters	Diorite ($\varepsilon'=5.8$, $\tan\delta=0.034\ 4$)[10]	Limestone ($\varepsilon'=6.7$, $\tan\delta=0.014\ 9$)[10]	Quartz ($\varepsilon'=4.0$, $\tan\delta=0.006\ 2$)[10]
Input power/mW	2.346 4	2.637 3	2.373 9
Radiated power/mW	2.346 4	2.637 3	2.373 9
Radiation efficiency/%	100	100	100
Linear gain/dBi	4.196 1	3.927 7	6.165 9
Coefficient of linear direction/dBi	10.492 1	9.716 2	12.411 2
3 dB beam bandwidth/(°)	(6.394, 56.900)	(14.795, 53.064)	(5.450, 53.482)

2.2.4 Effects of distances between heating cavity aperture and asphalt pavements on radiation performance

For a heating system made up of a magnetron, radiant heaters, air and asphalt composition, if impedance matching of the microwave source and the load end is achieved, microwave reflection will be greatly reduced, and, thereby, power coupling efficiency will be further increased. According to the generalized transmission-line theory, we will simplify the system to study impedance matching of microwave sources, and the simplified equivalent circuit is shown in Fig. 8. In the figure, the distance R from the microwave source to the heater radiation aperture and the distance h from the radiation aperture to the asphalt pavement are equivalent to two different characteristic impedances $Z_{in}(A)$ and $Z_{in}(B)$, respectively. $Z_{in}(C)=Z_L$ is the characteristic impedance of the asphalt mixture. The normalized input impedance from point B to the load can be indicated as

$$\overline{Z_{in}(B)}=\frac{Z_L+j\eta_0\tan(\beta h)}{\eta_0+jZ_0\tan(\beta h)} \tag{12}$$

where η_0 is the constant characteristic impedance of free air. The normalized input impedance from microwave source A to the load can be indicated as

$$\overline{Z_{in}(A)}=\frac{Z_{in}(B)+jZ_c\tan(\beta R)}{Z_c+jZ_{in}(B)\tan(\beta R)} \tag{13}$$

where Z_c is the equivalent characteristic impedance of the heater. Ideally, essential resistance Z_s of the microwave source must match with the input impedance at point A.

$$\overline{Z_s}=\overline{Z_{in}(A)}=\frac{Z_{in}(B)+jZ_c\tan(\beta R)}{Z_c+jZ_{in}(B)\tan(\beta R)} \tag{14}$$

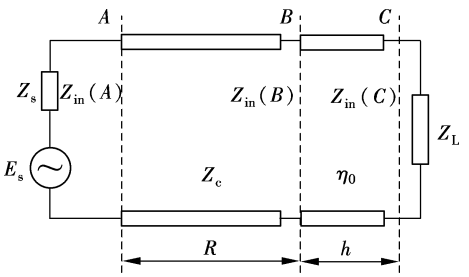

Fig. 8 Simplified equivalent circuit of microwave heating system

According to Eqs. (12) to (14), we know that for the same asphalt materials, i.e., the dielectric constant and the loss factor are invariant, in the same heating conditions, the height h from the heater to the asphalt road surface affects the impedance matching of the microwave source; that is to say, it affects the radiation effects of the microwave energy. Through appropriate adjustments of distance h between the radiation aperture of the heater surface and the asphalt pavement, the maximum radiation efficiency can be realized and the desired heating effects can be achieved.

Tab. 4 shows the radiation performance changes of heaters when the distance from the heating aperture to the road surface varies from 0 to 160 mm. It can be seen from Tab. 4 that when $h=0$ mm, the aperture is completely coated with road surface and the radiation efficiency is 82.8%, which is not the best. When $h=$ 0 to 60 mm, the radiated power values decrease; when $h=60$ mm or $h=120$ mm, the radiation efficiency reaches 100%, and the radiated power is higher than that of the other conditions; when the distance h exceeds 120 mm, the radiated power values decline gradually. Thus, according to actual work situations, when the distance from the aperture to the road surface remains between 60 and 120 mm, it is regarded that better heating effects can be obtained.

Tab. 4 Radiation performance of heating cavity of different distances from aperture to pavement

Pattern parameters	h/mm								
	0	20	40	60	80	100	120	140	160
Input power/mW	3.484 6	1.050 5	1.874 7	3.453 6	2.346 4	2.032 3	3.739 0	2.306 1	2.222 9
Radiated power/mW	2.887 2	1.050 5	1.874 7	3.453 6	2.346 4	2.032 3	3.739 0	2.306 1	2.222 9
Radiation efficiency/%	82.8	100	100	100	100	100	100	100	100
Linear gain/dBi	3.309 9	0.369 7	1.1340	5.867 1	4.196 1	2.847 0	5.733 2	3.658 0	3.264 5
Coefficient of linear direction/dBi	8.705 1	10.156 0	8.404 8	10.484 0	10.492 0	9.767 0	10.006 0	10.029 0	9.782 0
3 dB beam bandwidth/(°)	(10.406, 63.154)	(25.785, 63.950)	(27.147, 74.216)	(6.611, 50.884)	(6.394, 56.900)	(16.216, 54.347)	(6.373, 33.895)	(6.991, 40.384)	(7.263, 43.409)

3 Experimental Testing and Result Analysis

Experiments were carried out under four conditions, including $l=32.5$ mm, different aperture sizes, different horn electric lengths and different distances h. A 2M210F magnetron-tube with a working frequency of 2 455 MHz and a maximal output power of 875 W is used as the microwave source. Experimental installations are shown in Fig. 9. In the experiments, the safety of the operators is taken into account. And the metallic mesh enclosure is made to prevent

them from being radiated. An AV3941 radiometer is placed 0.5 m away from the experimental device to measure microwave leakage at the periphery of the device. The maximal microwave leakage is 67 $\mu W/cm^2$, indicating that the working environment is safe.

A grid template is made for measuring the temperature of the sample. The surface of the sample is divided into 8×10 grids. After heating 15 min, the temperatures are measured using an infrared thermometer[11].

Fig. 9 Microwave heating device

By using Matlab software, each of the measured temperature fields is fitted, and every fitting surface is shown in Fig. 10.

From the fitting results of the temperature fields as shown in Fig. 10, we can see that, compared with pyramidal horn heating, shortening of horn length results in a smoother temperature distribution curved surface of the asphalt mixtures, while the temperature at the periphery of the horn surface slightly decreases. In contrast, when the horn aperture size decreases, the average temperature of the asphalt mixtures increases, which is associated with more temperature variations and an apparent temperature ladder. A higher temperature zone appears in the left-middle portion, but the temperature rapidly decreases when deviating from this area. The right side of the horn aperture is almost not heated. When the distance between the horn aperture and the asphalt sample increases, the heating efficiency decreases, but the temperature uniformity is good. The experimental results are essentially consistent with the simulation results.

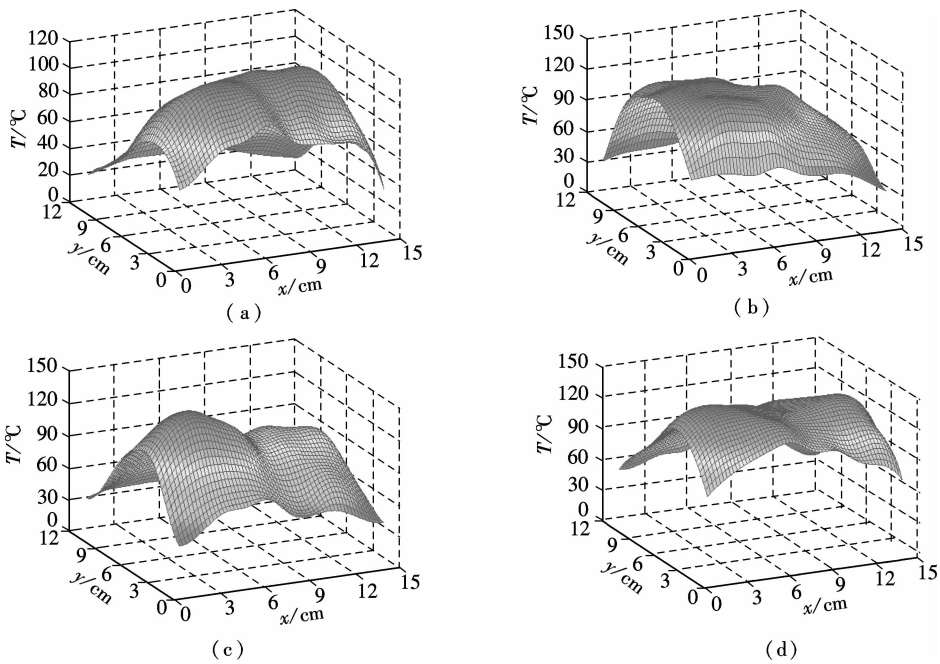

Fig. 10 Temperature field fitting of four conditions. (a) Basic type horn; (b) Shortened horn length; (c) Diminished surface size; (d) Extended distance

4 Conclusion

In this paper, two kinds of open-type microwave radiant heaters with different configurations are designed, and structural modeling and optimization of these heaters are carried out. The effects of the distance between the magnetron probe and the short-circuit board of the excitation cavity, different dielectric properties of different aggregates, the distance between the heater aperture and the pavement, different aperture sizes and horn electric lengths on heater radiation performance are studied, respectively. The asphalt mixture heating experiments under four different conditions are conducted, and the experimental results are consistent with the simulation results. It is confirmed that the developed microwave heater can result in better impedance matching and increase the heating efficiency of microwave radiation. All the results can provide a theoretical basis for the overall development and design of microwave pavement heating walls.

References

[1] Zhu Songqing, Shi Jinfei, Wang Hongxiang. Modeling and experiment of microwave heating for hot in-place recycling of asphalt pavements[J]. *Journal of Southeast University*: *Natural Science Edition*, 2006, **36**(3): 393 − 396. (in Chinese)

[2] Zhu Songqing, Shi Jinfei. Structural design and experimental research of microwave radiation heater for asphalt pavements [J]. *Journal of Southeast University*: *English Edition*, 2009, **25**(1): 68 − 73.

[3] Boyko L L, Lederer E H. Microwave road patch system

[C]//IEEE MTT-S International Microwave Symposium. Ottawa, Ont, Canada, 1978: 360 - 362.
[4] Pang Chuanxin, Yu Zhiyuan. Optimization design of the radiation device in a microwave system for asphalt heating [J]. *Vacuum Electronics*, 2007(2): 27 - 29. (in Chinese)
[5] Heriberto J D, Michael H T. Implementation of the pyramidal-horn antenna radiation-pattern equations using Mathcad [J]. *IEEE Antennas and Propagation Magazine*, 1999, **41** (5): 96 - 99.
[6] Chen Shaoping. Study about open microwave heater [J]. *Modern Electronics Technique*, 2006(7): 121 - 122, 125.
[7] Zeland Software, Inc. *IE3D manual* [M]. Fremont, CA, USA: Zeland Software, Inc., 2002
[8] Guan Denggao, Wang Shugen. The electromagnetic wave-absorbing properties of mineral materials and their application [J]. *Multipurpose Utilization of Mineral Resources*, 2006 (5): 17 - 21. (in Chinese)
[9] Hipple A V. *Dielectric materials and applications* [M]. Cambridge, MA, USA: The MIT Press, 1954: 63 - 74.
[10] Hopstock D M, Zanko L M. Minnesota taconite as a microwave-absorbing road aggregate material for deicing and pothole patching applications [J]. *Northland Transporter*, 2004 (3): 1 - 16.
[11] Cuccurullo G, Berardi P G, Carfagna R, et al. IR temperature measurement in microwave heating [J]. *Infrared Physics and Technology*, 2002, **43**(3/4/5): 145 - 150.

沥青路面微波加热器电磁仿真与实验分析

朱松青[1,2] 张志胜[1] 史泰龙[3]

([1] 东南大学机械工程学院, 南京 211189)
([2] 南京工程学院自动化学院, 南京 211167)
([3] 东南大学信息科学与工程学院, 南京 211189)

摘要:为了研究微波加热再生沥青路面时的热电效率和再生温度分布的均匀性,设计了一种波导激励腔,并应用于微波加热器的结构设计. 运用波导传输线理论, 确定了激励腔的结构尺寸. 采用 IE3D 分别对磁控管探头(天线)与短路板间距、不同喇叭长度和口面尺寸、不同沥青混合料介电性能和加热腔口面与沥青路面不同距离 4 种情况进行了电磁仿真. 结果表明:磁控管探头离短路板距离 32.5 mm 时为最佳安装位置;天线长度缩短是改善加热均匀性的主要因素;当集料为石灰石时,其加热效果最好;通过调整加热器辐射口面与沥青路面间距,可实现最大辐射效率. 通过对 4 种不同情况的沥青混合料进行加热实验,得到了与仿真基本一致的结果,证实开发设计的微波加热器能够较好地实现阻抗匹配,从而提高了热再生质量和效率.

关键词:微波加热器;谐振激励腔;结构设计;电磁仿真;温度场分布;实验分析
中图分类号: TM15